

Alkylammonium bis(trifluoromethylsulfonyl)imide as a dopant in the hole-transporting layer for efficient and stable perovskite solar cells

Youngwoong Kim^{a, †}, Geunjin Kim^{a, †}, Eun Young Park^a, Chan Su Moon^a, Seung Joo Lee^a, Jason J. Yoo^a, Seongsik Nam^{a, b}, Jino Im^c, Seong Sik Shin^{a, b}, Nam Joong Jeon^{a, *}, and Jangwon Seo^{a, d, *}

^aDivision of Advanced Materials, Korea Research Institute of Chemical Technology (KRICT), Daejeon 34114, Republic of Korea

^bSKKU Advanced Institute of Nanotechnology (SAINT) and Department of Nanoengineering, Sungkyunkwan University, Suwon 16419, Republic of Korea

^cChemical Data-Driven Research Center, Korea Research Institute of Chemical Technology (KRICT), Daejeon 34114, Republic of Korea

^dDepartment of Chemical and Biomolecular Engineering, Korea Advanced Institute of Science and Technology (KAIST), Daejeon 34141, Republic of Korea

[†]Y. Kim and G. Kim contributed equally to this work.

Email: njjeon@kRICT.re.kr, jwseo@kaist.ac.kr

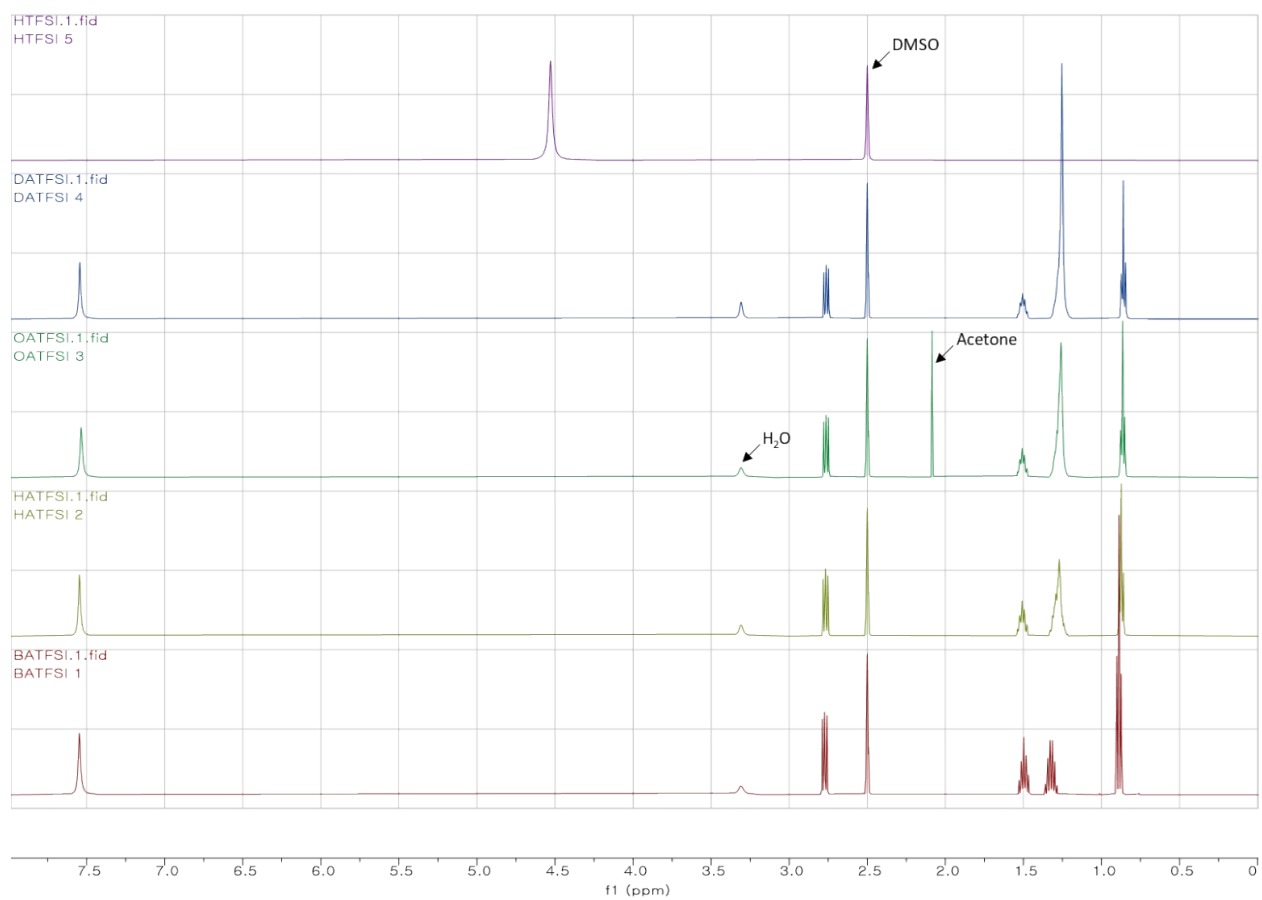


Fig. S1. ¹H NMR spectrum of ionic liquid dopants

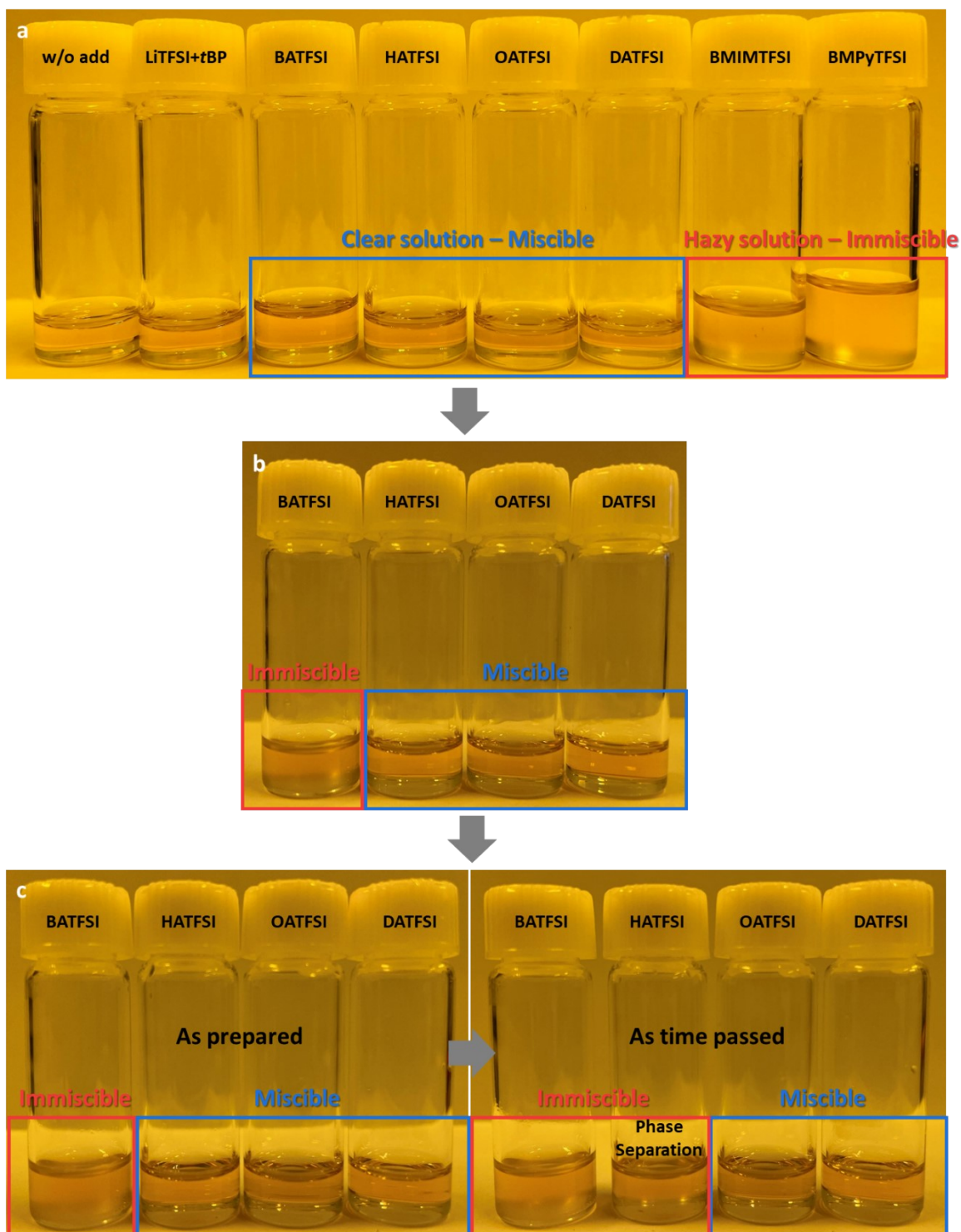


Fig. S2. Photographs of PTAA solutions (a) without dopant or with LiTFSI+tBP and 9.75 mM of IL dopants, (b) 24.37 mM of IL dopants, and (c) 80.41 mM of IL dopants

Dopant concentration (mM) ^a	BATFSI	HATFSI	OATFSI	DATFSI
9.75	O	O	O	O
24.37	X	O	O	O
60.92	X	O	O	O
80.41	X	X	O	O
121.84	X	X	O	O
243.67	X	X	O	O
304.59	X	X	X	X

Table S1. Miscibility test of alkylammonium TFSIs in PTAA solutions

^aThe solutions are also containing PTAA at 10mg ml⁻¹.

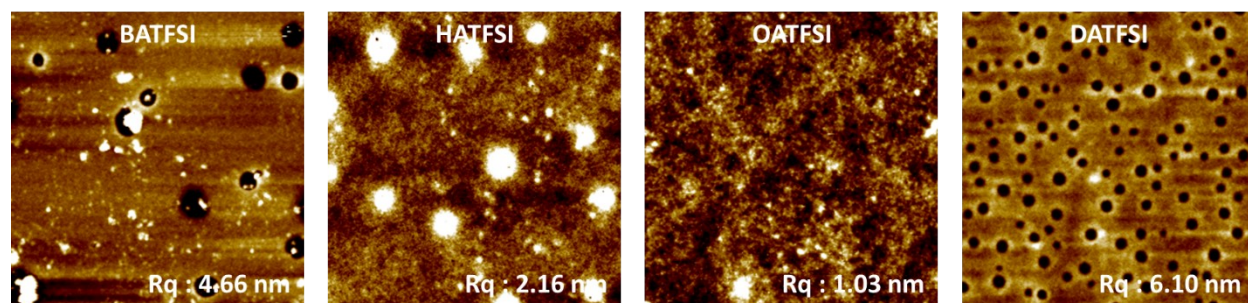


Fig. S3. AFM images (5 $\mu\text{m} \times 5 \mu\text{m}$) of PTAA containing the same concentration of alkylammonium TFSI dopants with different alkyl chain lengths

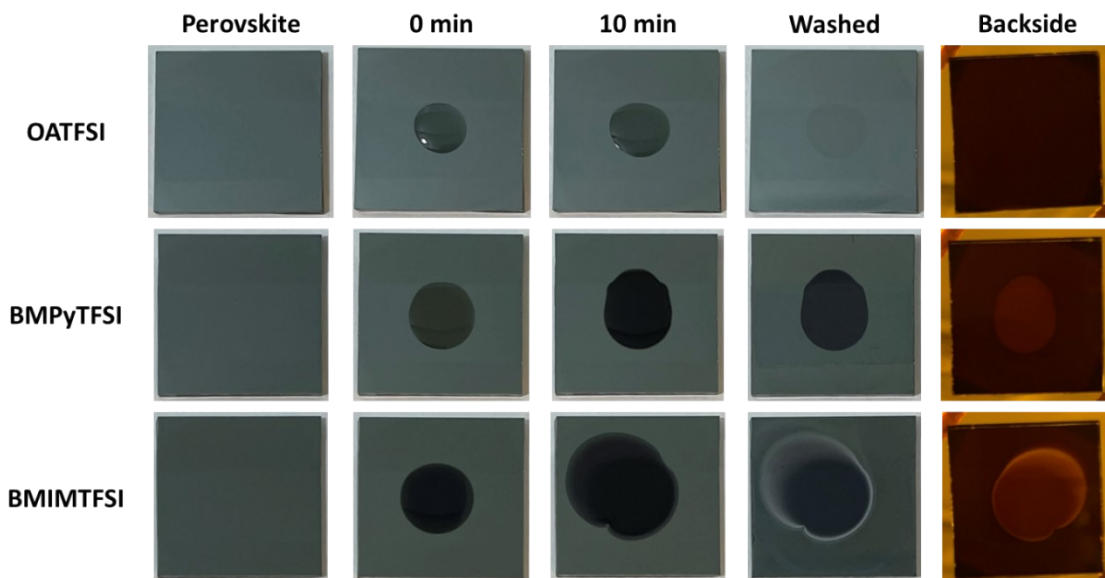


Fig. S4. Photographs of perovskite layers with droplets of OATFSI, BMPyTFSI, and BMIMTFSI

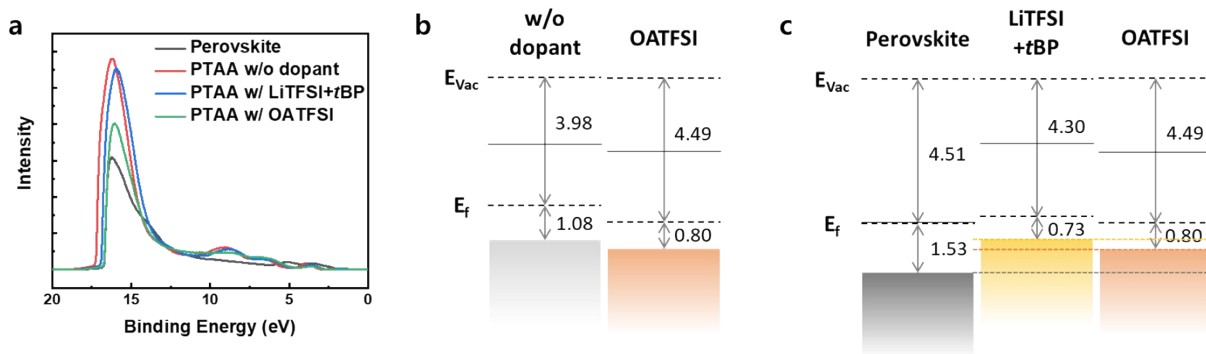


Fig. S5. (a) UPS spectra for perovskite, PTAA with or without various dopants, (b) change of energy level for PTAA in present/absence of OATFSI, and (c) energy level alignments of perovskite and PTAA with LiTFSI+tBP or OATFSI.

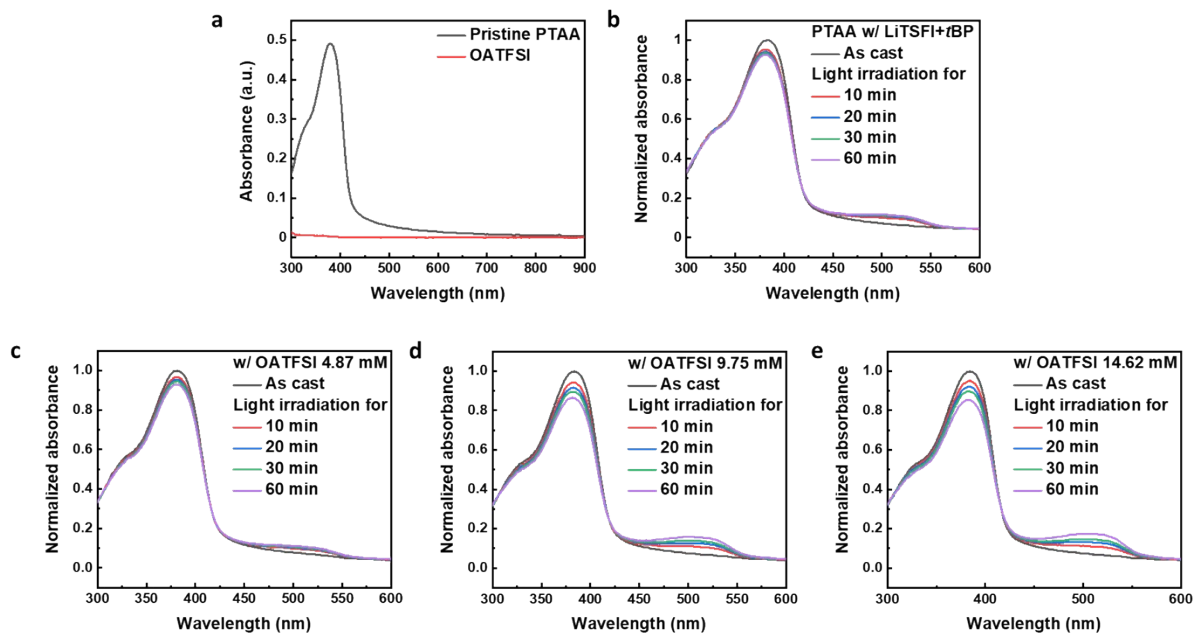


Fig. S6. UV-vis spectra of (a) pristine PTAA in film state (prepared from 10 mg ml⁻¹ of PTAA solution in toluene) and pristine OATFSI in solution state (9.75 mM of OATFSI in toluene) and change of UV-Vis absorption spectra for (b) PTAA film with LiTFSI+tBP and (c-e) PTAA films with various dopant concentrations of OATFSI under illumination

Table S2. Electrical property of pristine PTAA film, PTAA film with LiTFSI+tBP, and PTAA films with various dopant concentrations of OATFSI

Dopant	Conductivity (S cm ⁻¹)
w/o additive	1.41×10 ⁻⁷
LiTFSI+tBP	2.99×10 ⁻⁵
OATFSI 4.87 mM	3.28×10 ⁻⁵
OATFSI 9.75 mM	1.06×10 ⁻⁴
OATFSI 14.62 mM	1.22×10 ⁻⁴

Dopant Concentration ^a	Scan Direction	V_{OC} (V)	J_{SC} (mA cm ⁻²)	FF	PCE _{max} (%) (PCE _{avg} (%))	R_s (Ω·cm ²)	R_{sh} (kΩ·cm ²)
0 mM	Rev.	0.884	25.29	0.335	7.50 (7.12)	984.71	16.57
	Fwd.	0.836	25.09	0.256	5.36 (5.16)	1210.00	1.22
2.44 mM	Rev.	0.985	25.82	0.796	20.24 (20.14)	33.04	27.07
	Fwd.	0.928	25.84	0.685	16.43 (16.34)	69.32	68.17
4.87 mM	Rev.	0.997	25.41	0.803	20.34 (20.20)	31.59	28.02
	Fwd.	0.952	25.39	0.715	17.27 (17.32)	61.03	33.77
7.31 mM	Rev.	0.997	25.53	0.810	20.63 (20.35)	27.75	3410.00
	Fwd.	0.962	25.48	0.748	18.33 (17.99)	43.07	117.4
9.75 mM	Rev.	1.028	25.60	0.822	21.63 (21.31)	23.20	725.32
	Fwd.	0.993	25.55	0.775	19.65 (19.49)	33.79	294.01
12.18 mM	Rev.	1.030	25.61	0.818	21.57 (21.07)	24.21	21.32
	Fwd.	0.997	25.61	0.777	19.84 (19.32)	33.42	39.96
14.62 mM	Rev.	1.036	25.17	0.793	20.69 (20.03)	25.28	39.96
	Fwd.	0.948	25.08	0.723	17.19 (16.63)	44.57	32.50

Table S3. Photovoltaic properties of PSCs using different dopant concentrations of OATFSI

^a) Devices were fabricated without surface treatment on mp-TiO₂

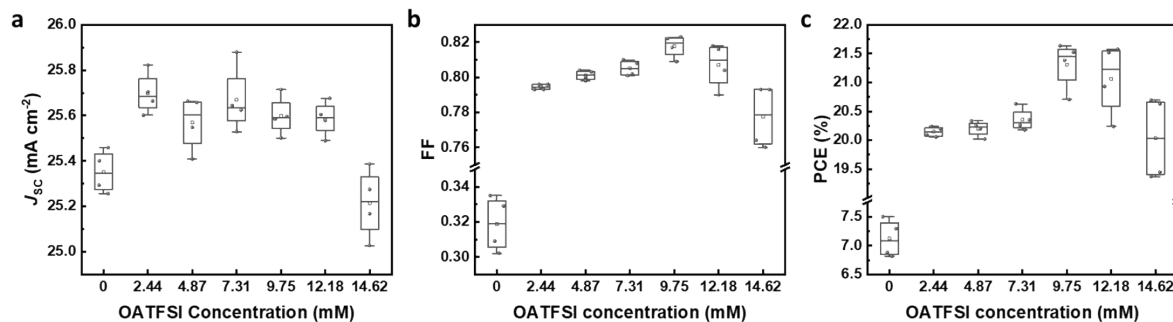


Fig. S7. (a) J_{SC} , (b) FF, and (c) PCE statistics in box-and-whisker plots (center line: median, box limits: upper and lower quartiles, whiskers: 1.5× interquartile range, points: outliers) of PSCs using different dopant concentrations of OATFSI

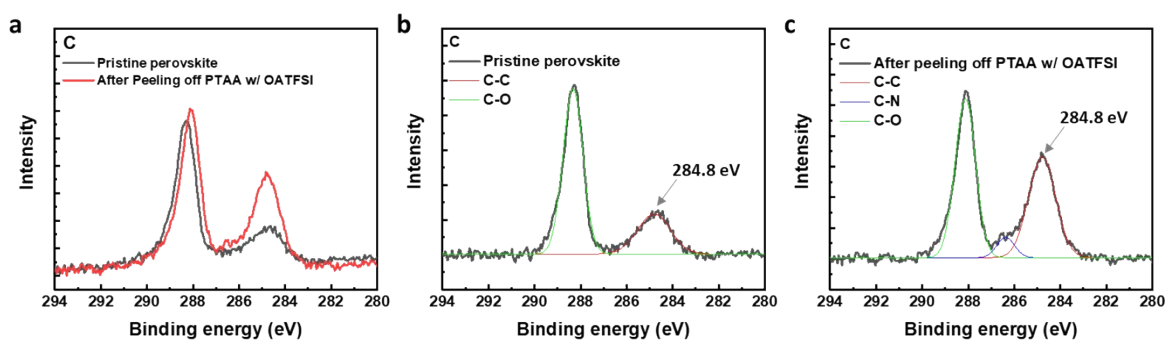
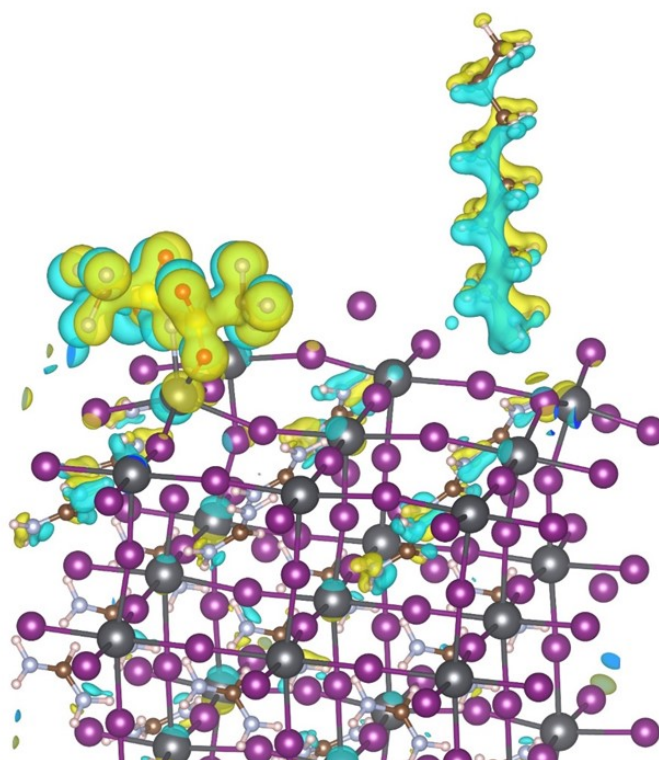


Fig. S8. XPS spectra of (a) pristine perovskite layer and perovskite layer after peeling off PTAA film using 9.75 mM of OATFSI with (b-c) the detailed fitting curves

OA + TFSI on PbI_2 termination



$$\Delta E_{\text{Binding}} = -5.62 \text{ eV}$$

Fig. S9. DFT calculation for interaction between the OATFSI and perovskite

OATFSI Concentration ^a	Surface Treatment	Scan Direction	V_{OC} (V)	J_{SC} (mA cm ⁻²)	FF	PCE _{max} (%) (PCE _{avg} (%))
4.87 mM	X	Rev.	1.007	25.11	0.816	20.62 (20.00)
		Fwd.	0.981	25.12	0.785	19.34 (18.68)
9.75 mM	X	Rev.	1.073	25.00	0.833	22.37 (21.93)
		Fwd.	1.022	24.97	0.801	20.44 (20.02)
4.87 mM	O	Rev.	1.036	25.01	0.822	21.31 (20.93)
		Fwd.	0.999	24.95	0.796	19.85 (19.43)
9.75 mM	O	Rev.	1.087	24.89	0.839	22.70 (22.25)
		Fwd.	1.034	24.83	0.796	20.42 (20.10)

Table S4. Photovoltaic properties of PSCs before/after surface treatment using OATFSI

^a) Devices were fabricated with surface treatments on mp-TiO₂ using strontium bis(trifluoromethylsulfonyl)imide. Similar to surface treatments using salt materials on ETLs, surface treatment using strontium bis(trifluoromethylsulfonyl)imide was used to improve the performance of PSCs.¹⁻⁴

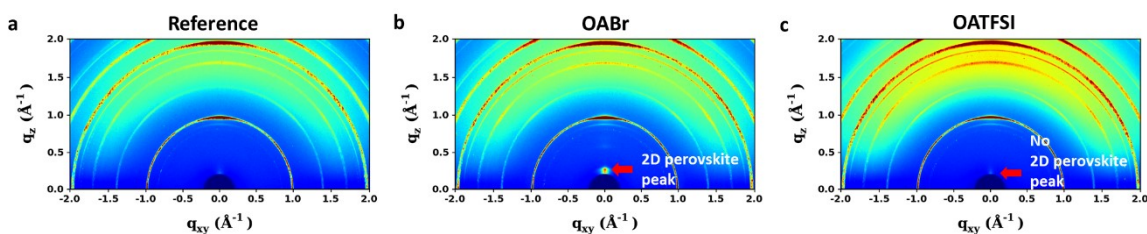


Fig. S10. GIWAXS patterns of (a) pristine perovskite, (b) octylammonium bromide (OABr)-treated perovskite, and (c) octylammonium TFSI (OATFSI)-treated perovskite. To obtain surface crystalline profile for the corresponding samples, the incidence angle of the X-ray beam was set to 0.10°

	Sample 1 decay time (μs)	Sample 2 decay time (μs)	Sample 3 decay time (μs)	Average decay time (μs)
Pristine perovskite on quartz	6.1	5.3	-	5.7
Perovskite w/ OATFSI surface treatment	9.7	10.0	-	9.8
PTAA w/ OATFSI 4.87 mM ^a	13.2	11.9	13.6	12.9
PTAA w/ OATFSI 9.75 mM ^a	27.7	30.9	30.0	29.5
PTAA w/ LiTFSI+tBP ^a	10.3	10.3	11.3	10.6

Table S5. Summary of long component of lifetime extracting from TCSPC curves

^a)Perovskite layers were not treated with OATFSI

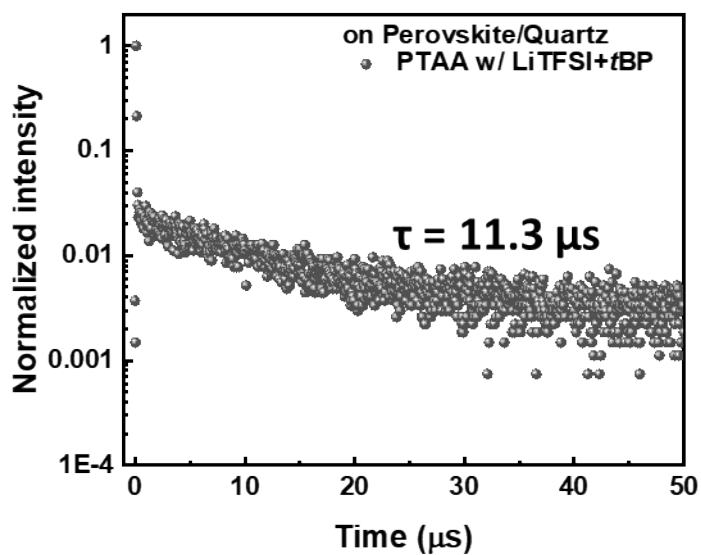


Fig. S11. PL transients of perovskite covered by PTAA with LiTFSI+tBP

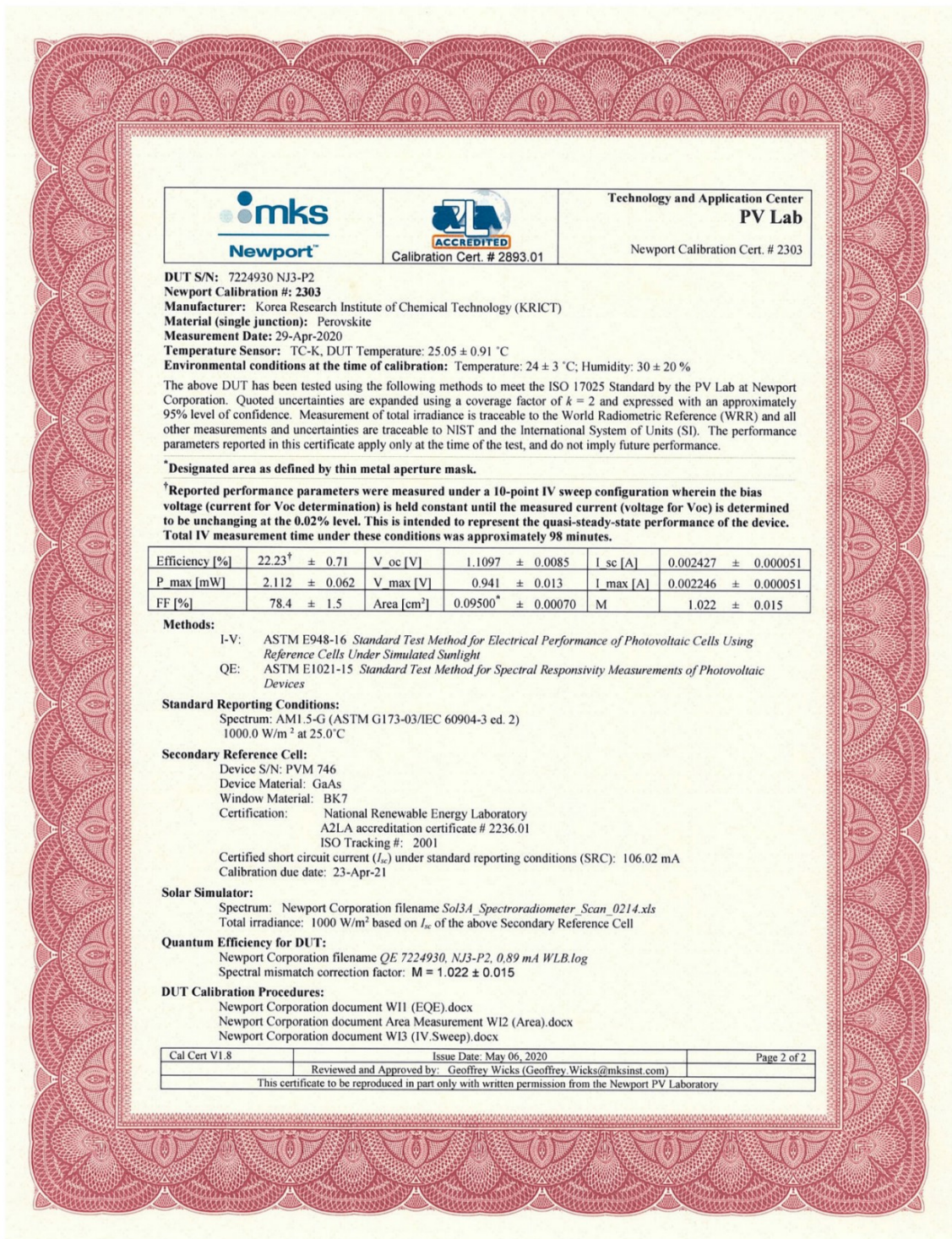


Fig. S12. (Continued on next page) Certification of OATFSI-based PSC exhibiting QSS PCE of 22.23%

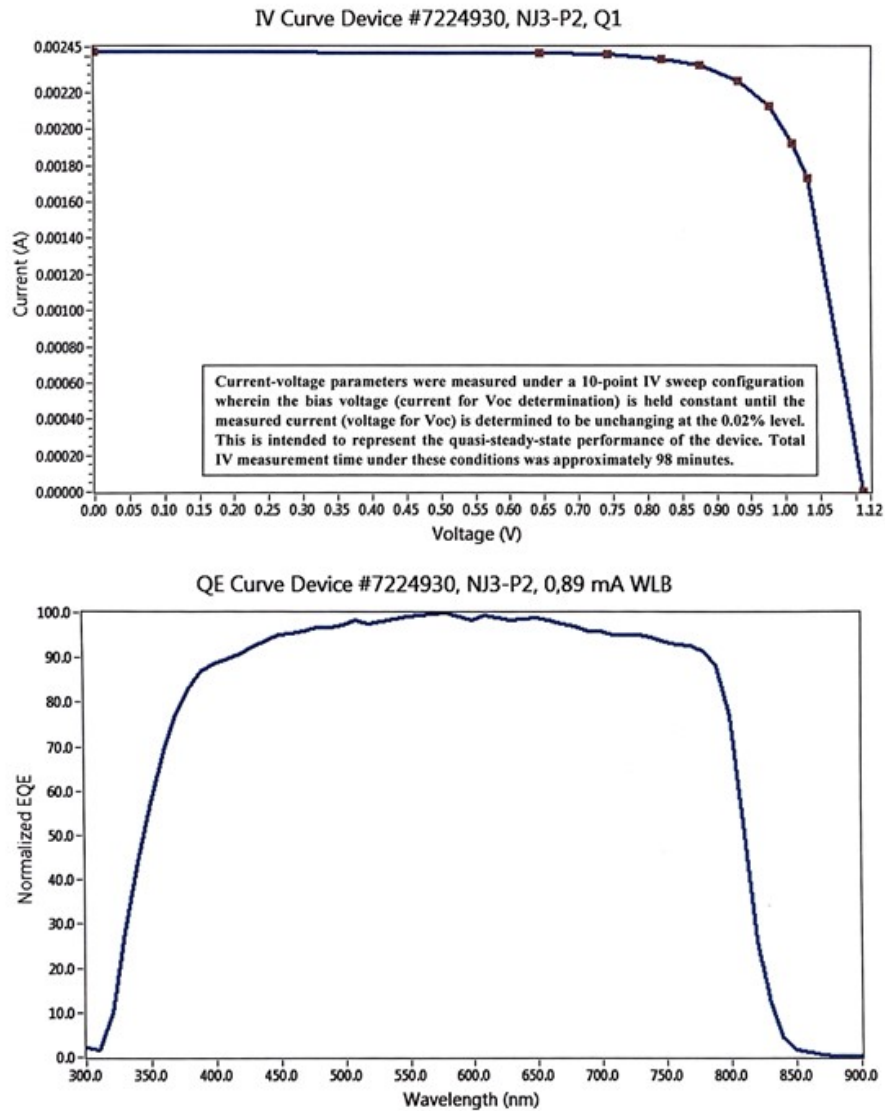


Fig. S12. (Continued on next page) Certification of OATFSI-based PSC exhibiting QSS PCE of 22.23%

Table S6. Summary of the certified performances (with PCE of over 22%) for PTAA-based PSCs reported to date

No.	Structure	Measurement Method	Certified PCE (%)	dopant	Reference
This work	n-i-p	QSS measurement	22.2	OATFSI	-
1	n-i-p	Reverse/Forward measurement	22.1	LiTFSI+tBP	<i>Science</i> 2017 , 356, 1376-1379
2	n-i-p	Reverse/Forward measurement	23.9	F4TCNQ+LiHFDF	<i>Science</i> 2022 , 377, 1227-1232
3	p-i-n	QSS measurement	22.3	X	<i>Nat. Energy</i> 2020 , 5, 131-140
4	p-i-n	Reverse/Forward measurement	22.8	X	<i>J. Am. Chem. Soc.</i> 2020 , 142, 20134-20142
5	p-i-n	Reverse/Forward measurement	24.3	X	<i>Science</i> 2022 , 376, 416-420

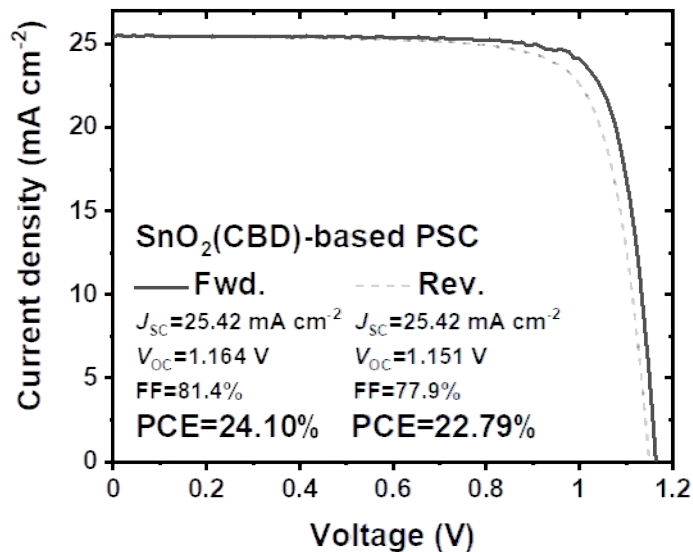


Fig. S13. J - V curve for CBD SnO₂-based PSC

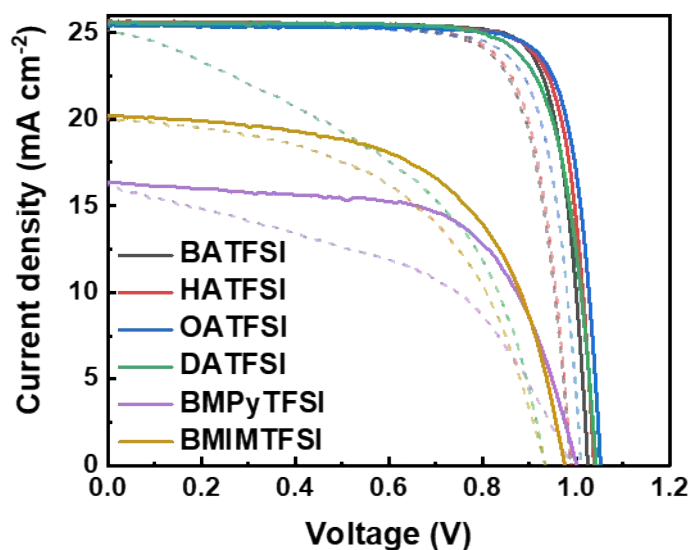


Fig. S14. J - V curves of PSCs using the same concentration of alkylammonium TFSIs with different alkyl chain lengths and commercial ionic liquid dopants

Table S7. Photovoltaic properties of PSCs using the same concentration of alkylammonium TFSIs with different alkyl chain lengths and commercial ionic liquid dopants

Dopant ^a	Scan Direction	V_{oc} (V)	J_{sc} (mA cm^{-2})	FF	PCE_{max} (%) (PCE_{avg} (%))
BATFSI	Rev.	1.026	25.63	0.821	21.59 (21.10)
	Fwd.	0.991	25.59	0.768	19.47 (18.51)
HATFSI	Rev.	1.039	25.65	0.814	21.69 (21.27)
	Fwd.	0.993	25.57	0.775	19.67 (19.33)
OATFSI	Rev.	1.052	25.41	0.819	21.91 (21.38)
	Fwd.	1.013	25.43	0.785	20.24 (19.54)
DATFSI	Rev.	1.043	25.56	0.784	20.90 (20.00)
	Fwd.	0.936	25.11	0.462	10.85 (11.57)
BMPyTFSI	Rev.	1.002	16.34	0.640	10.47 (6.62)
	Fwd.	0.994	16.18	0.471	7.57 (3.64)
BMIMTFSI	Rev.	0.976	20.17	0.592	11.66 (9.52)
	Fwd.	0.937	19.94	0.530	9.90 (7.90)

^aDevices were fabricated with surface treatments on mp-TiO₂ using strontium bis(trifluoromethylsulfonyl)imide.

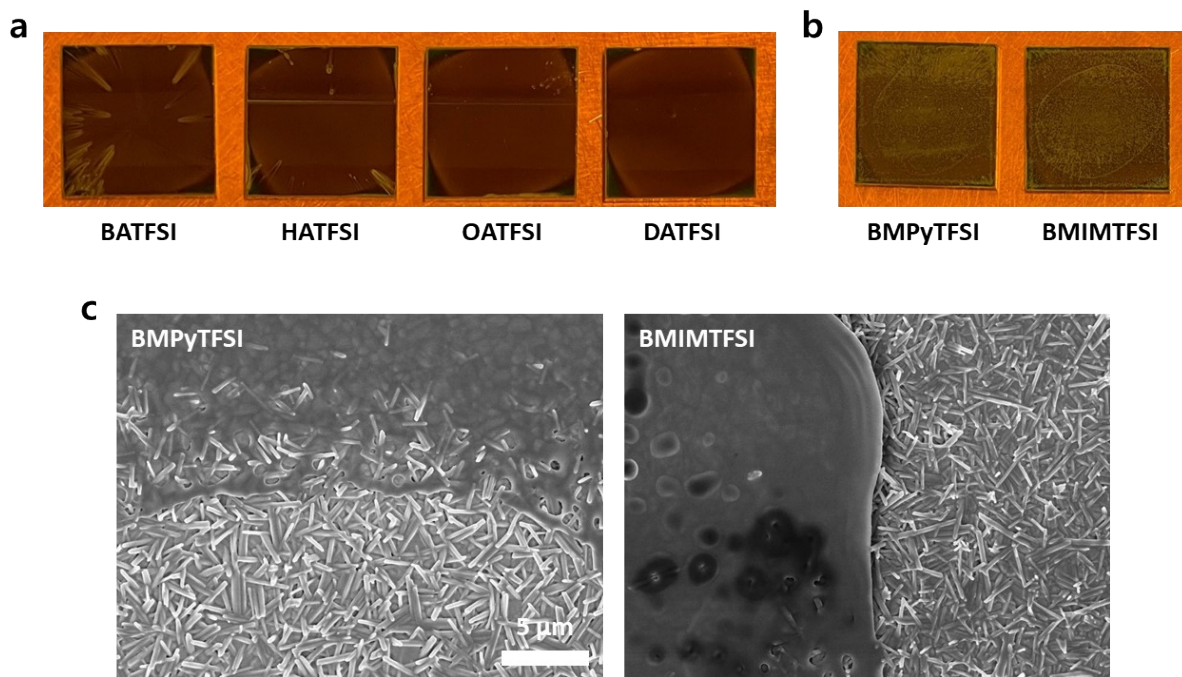


Fig. S15. Photographs of (a) HTLs containing alkylammonium TFSIs with different alkyl chain lengths and (b) HTLs containing commercial ionic liquid dopants on the perovskite layers; (c) SEM images of HTLs containing commercial ionic liquid dopants on the perovskite layers

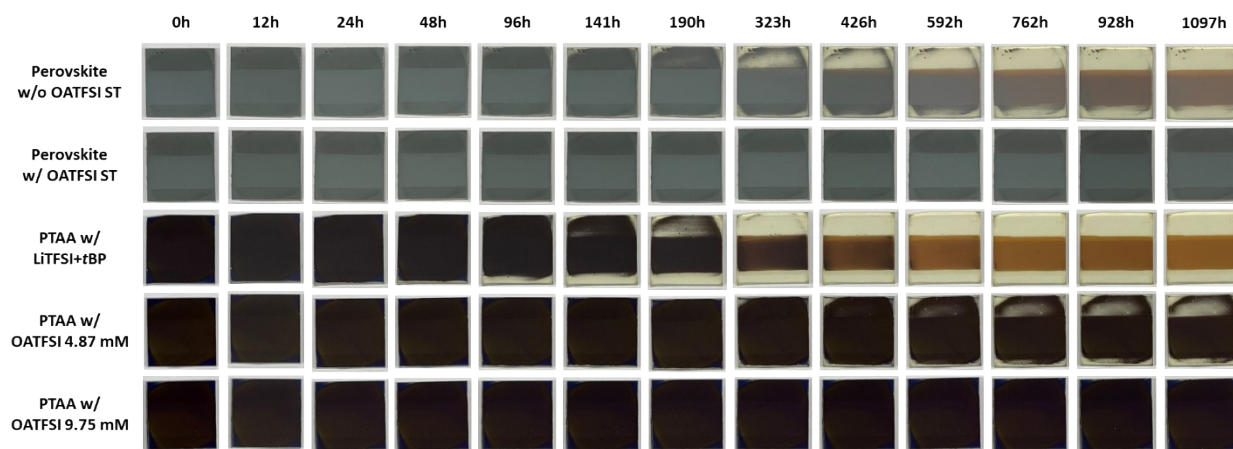


Fig. S16. Photographs of changes for perovskite films with and without surface treatment using OATFSI and perovskite films covered by PTAAAs doped by OATFSI and LiTFSI+tBP at 40~55% RH

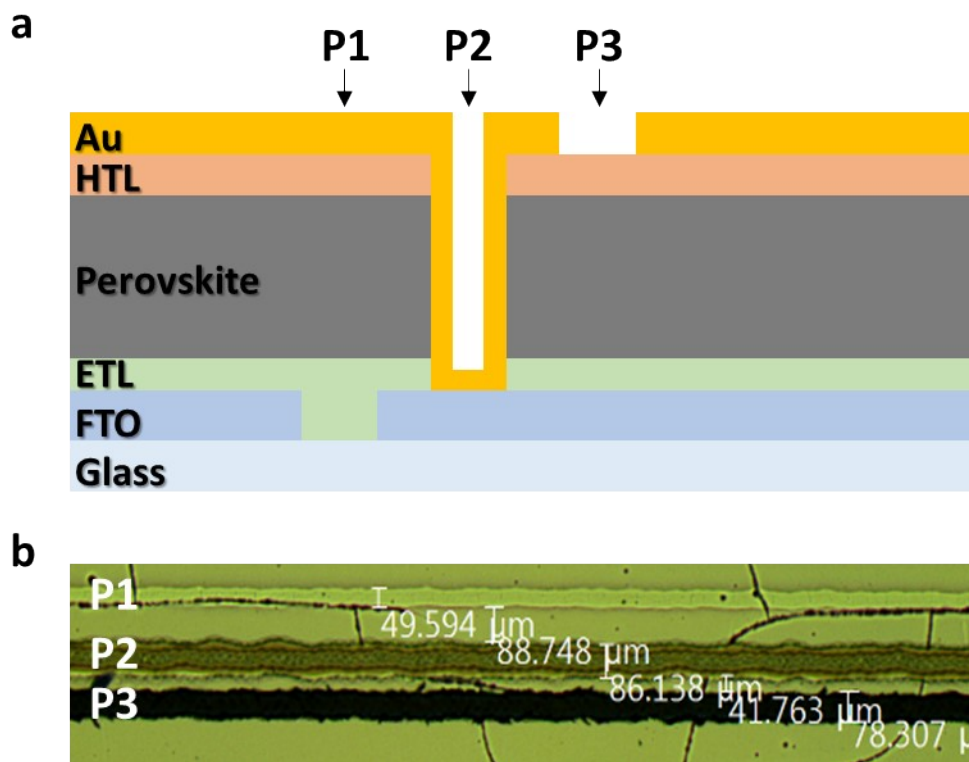


Fig. S17. (a) Schematic and (b) optical microscope image of P1, P2, and P3 interconnection lines of the module

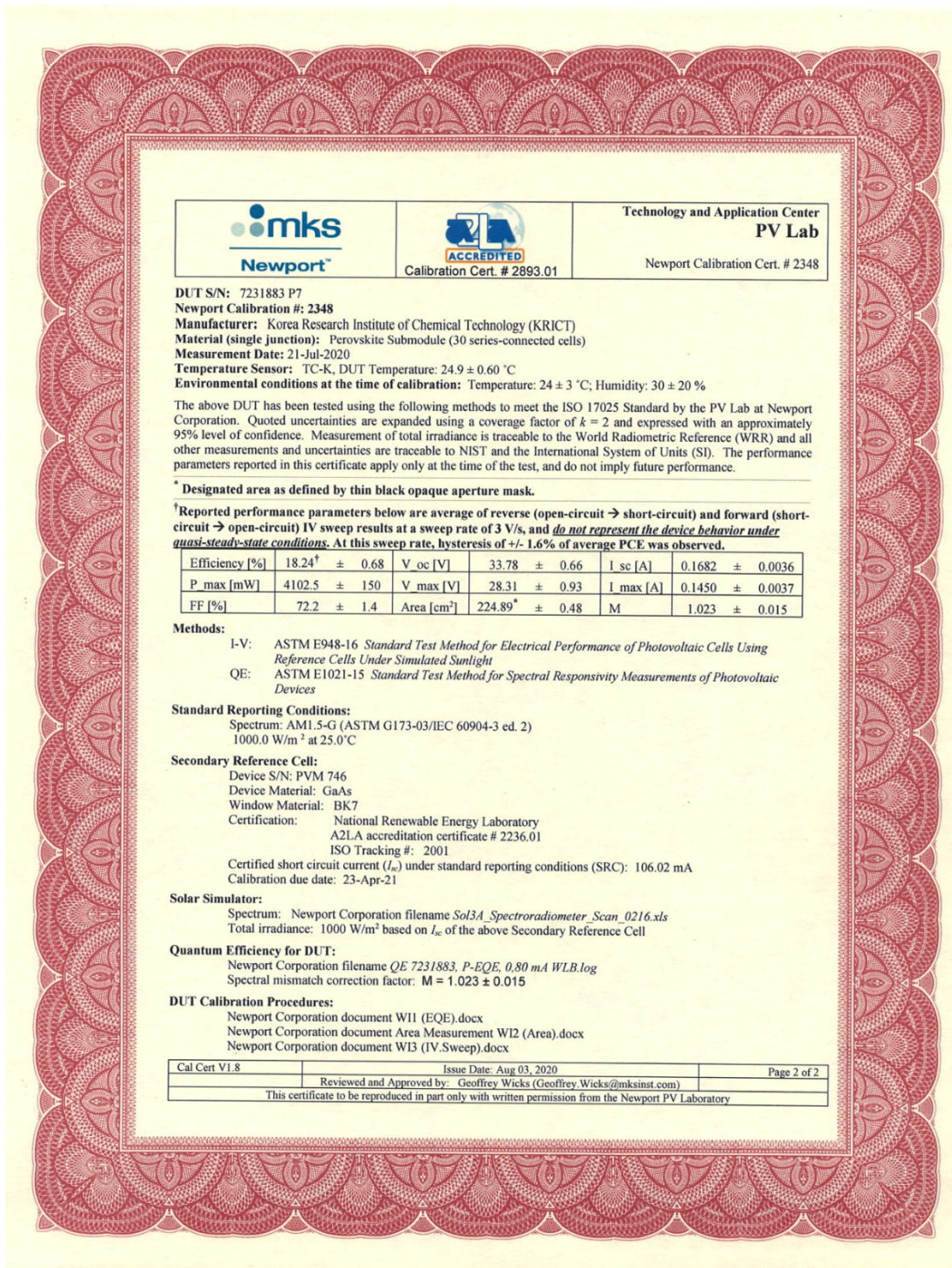


Fig. S18. Certification of OATFSI-based perovskite module exhibiting PCE of 18.24%

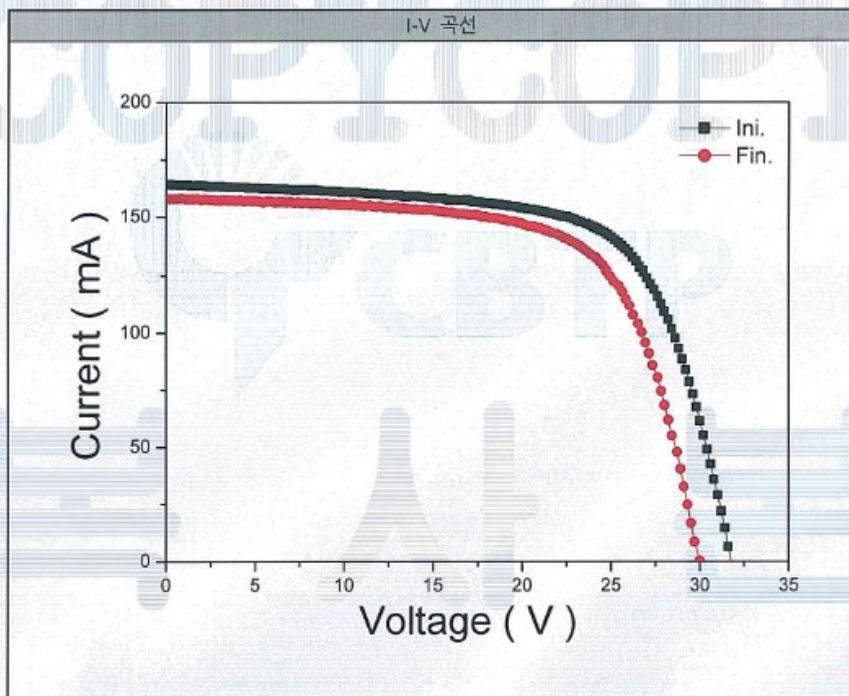
Table S8. Photovoltaic parameters of the perovskite modules using OATFSI

No.	J_{sc} (mA cm ⁻²)	V_{oc} (V)	FF (%)	PCE in aperture area (225 cm ²) (%)
1	0.72	31.4	77.8	17.6
2	0.69	31.3	74.5	16.2
3	0.70	30.9	69.3	15.0
4	0.70	31.4	72.0	15.7
5	0.67	30.8	77.0	16.1
6	0.72	31.9	76.2	17.5
7	0.69	31.3	75.2	16.2
8	0.71	32.6	78.2	18.2
9	0.69	30.6	73.4	15.5
10	0.72	32.6	79.7	18.6
11	0.71	31.0	74.1	16.2
12	0.72	31.2	77.0	17.0
13	0.72	30.9	74.6	16.7
14	0.68	30.5	72.1	15.0
15	0.73	33.0	80.0	19.2
16	0.70	32.7	76.1	17.5
17	0.73	32.7	73.2	17.6
18	0.75	32.1	76.8	18.4
19	0.71	32.3	79.9	18.3
20	0.72	32.3	78.2	18.2
21	0.71	32.2	80.0	18.4
22	0.71	32.8	79.7	18.7
23	0.71	33.2	82.0	19.4
24	0.71	31.1	77.4	17.2
Average	0.7105±0.0174	31.83±0.84	76.46±3.11	17.30±1.30

4.2 시험결과

1) I-V 특성 평가

구분	Voc (V)	Isc (mA)	J _{sc} (mA/cm ²)	FF (%)	Power (W)	Eff (%)	비고	
#1	Ini. (0 h)	31.80	164.23	0.729	67.49	3.52	15.66	225 cm ²
	Fin. (1 000h)	29.96	158.00	0.702	67.28	3.19	14.16	
	rate (%)	-5.79	-3.79	-3.70	-0.31	-9.38	-9.58	



-끝-

Fig. S19. Result of outsourcing damp heat test for OATFSI-based perovskite module before and after 1000 h

Supplemental references

1. M. Kim, I.-w. Choi, S. J. Choi, J. W. Song, S.-I. Mo, J.-H. An, Y. Jo, S. Ahn, S. K. Ahn, G.-H. Kim and D. S. Kim, *Joule*, 2021, **5**, 659-672.
2. X. Liu, Y. Zhang, L. Shi, Z. Liu, J. Huang, J. S. Yun, Y. Zeng, A. Pu, K. Sun, Z. Hameiri, J. A. Stride, J. Seidel, M. A. Green and X. Hao, *Adv. Energy Mater.*, 2018, **8**, 1800138.
3. D. Liu, S. Li, P. Zhang, Y. Wang, R. Zhang, H. Sarvari, F. Wang, J. Wu, Z. Wang and Z. D. Chen, *Nano Energy*, 2017, **31**, 462-468.
4. F. Giordano, A. Abate, J. P. Correa Baena, M. Saliba, T. Matsui, S. H. Im, S. M. Zakeeruddin, M. K. Nazeeruddin, A. Hagfeldt and M. Graetzel, *Nat. Commun.*, 2016, **7**, 10379.